J Mol Neurosci (2017) 62:329–343
DOI 10.1007/s12031-017-0941-x

Glial and Neuronal Protein Tyrosine Phosphatase Alpha (PTPα) Regulate Oligodendrocyte Differentiation and Myelination

Yuda Shih[1,2,3] · Philip T. T. Ly[4,2,3] · Jing Wang[4,3] · Catherine J. Pallen[1,4,2,3]

Received: 12 April 2017 / Accepted: 8 June 2017 / Published online: 24 June 2017

Abstract CNS myelination defects occur in mice deficient in receptor-like protein tyrosine phosphatase alpha (PTPα). Here, we investigated the role of PTPα in oligodendrocyte differentiation and myelination using cells and tissues from wild-type (WT) and PTPα knockout (KO) mice. PTPα promoted the timely differentiation of neural stem cell-derived oligodendrocyte progenitor cells (OPCs). Compared to WT OPCs, KO OPC cultures had more NG2+ progenitors, fewer myelin basic protein (MBP)+ oligodendrocytes, and reduced morphological complexity. In longer co-cultures with WT neurons, more KO than WT OPCs remained NG2+ and while equivalent MBP+ populations of WT and KO cells formed, the reduced area occupied by the MBP+ KO cells suggested that their morphological maturation was impeded. These defects were associated with reduced myelin formation in KO OPC/WT neuron co-cultures. Myelin formation was also impaired when WT OPCs were co-cultured with KO neurons, revealing a novel role for neuronal PTPα in myelination. Canonical Wnt/β-catenin signaling is an important regulator of OPC differentiation and myelination. Wnt signaling activity was not dysregulated in OPCs lacking PTPα, but suppression of Wnt signaling by the small molecule XAV939 remediated defects in KO oligodendrocyte differentiation and enhanced myelin formation by KO oligodendrocytes. However, the myelin segments that formed were significantly shorter than those produced by WT oligodendrocytes, raising the possibility of a role for glial PTPα in myelin extension distinct from its pro-differentiating actions. Altogether, this study reveals PTPα as a molecular coordinator of oligodendroglial and neuronal signals that controls multiple aspects of oligodendrocyte development and myelination.

Keywords Protein tyrosine phosphatase alpha · Oligodendrocyte maturation · Myelination · Remediation

Yuda Shih and Philip T. T. Ly contributed equally to this work.

Electronic supplementary material The online version of this article (doi:10.1007/s12031-017-0941-x) contains supplementary material, which is available to authorized users.

✉ Catherine J. Pallen
cpallen@mail.ubc.ca

[1] Department of Pathology and Laboratory Medicine, University of British Columbia, Vancouver, BC, Canada

[2] International Collaboration on Repair Discoveries, University of British Columbia, Vancouver, BC, Canada

[3] BC Children's Hospital Research Institute, University of British Columbia, 950 West 28th Ave, Vancouver, BC V5Z 4H4, Canada

[4] Department of Pediatrics, University of British Columbia, Vancouver, BC, Canada

Introduction

CNS myelination is accomplished by oligodendrocytes (OLs) and is crucial for proper nervous system function in vertebrates. During CNS development, oligodendrocyte progenitor cells (OPCs) differentiate into OLs, a process characterized by profound changes in gene expression and cell morphology. Neuron-OPC and neuron-OL contacts and signaling orchestrate OL development, myelin growth, and multi-layered wrapping of the axon by the extended plasma membrane of the OL (Bercury and Macklin 2015; Maldonado and Angulo 2014; Simons and Trajkovic 2006). The establishment of a compact, segmented myelin sheath regulates the molecular organization and function of the axon, as well as preventing

axonal degeneration (Buttermore et al. 2013; Chang and Rasband 2013; Lee et al. 2012; Nave 2010; Nave and Werner 2014). Not surprisingly, myelin defects or damage can result in profound cognitive and motor impairments. Remediation of the acquired myelin destruction that occurs in diseases such as multiple sclerosis is a key therapeutic goal that will be accelerated by improved understanding of the complex molecular and cellular processes that regulate the multi-step process of myelination.

Reversible protein tyrosine phosphorylation, mediated by protein tyrosine kinases (PTKs) and phosphatases (PTPs), is a central mechanism of molecular regulation that governs numerous cell processes in development, including myelination. PTP alpha (PTPα) is a transmembrane receptor-type phosphatase with enriched expression in brain (Sap et al. 1990), and PTPα-null mice have defective CNS and PNS myelination (Tiran et al. 2006; Wang et al. 2009). The absence of PTPα in the CNS results in increased numbers of OL lineage cells in the embryonic forebrain, and impairs the maturation of OPCs into myelin-forming OLs that is consistent with decreased myelin basic protein (MBP) expression in the developing brain. Our previous studies have revealed that PTPα plays two roles in OPCs: limiting OPC proliferation and inducing cell cycle exit, and promoting differentiation. In accord with a major physiological role of PTPα as an activator of Src family tyrosine kinases (SFKs) (Pallen 2003; Ponniah et al. 1999; Su et al. 1999), PTPα activates the SFK Fyn in proliferating OPCs to suppress Ras and Rho, with upregulated expression of the cell cycle exit regulator p27 Kip1 mediated by Rho suppression (Wang et al. 2012). When OPCs are induced to differentiate in vitro, PTPα responds by activating Fyn and the Fyn downstream effectors FAK, Rac, and Cdc42 while inhibiting Rho (Wang et al. 2009). Without PTPα, OPCs do not differentiate properly, suggesting that this is a major impediment to effective CNS myelination in PTPα-null mice.

In this study, we established model systems of varying complexity to interrogate the role of PTPα in the stages and cell types involved in myelination, using organotypic cerebellar slice cultures, neural stem cell (NSC)-derived OPC cultures, and myelinating OPC/neuron co-cultures sourced from cell and tissues of wild-type (WT) and PTPα-null (KO) mice. We also investigated canonical Wnt/β-catenin signaling as a first step towards determining how PTPα pro-differentiation signaling intersects with other key pathways that regulate OL differentiation. Altogether, our findings show that the absence of oligodendroglial PTPα delays the differentiation and morphological maturation of OLs in a manner independent of Wnt/β-catenin signaling, reveals a potential role for oligodendroglial PTPα in promoting myelin extension, and demonstrates a novel neuronal requirement for PTPα in myelination.

Materials and Methods

Animals Animal care and use followed the guidelines of the University of British Columbia (UBC) and the Canadian Council on Animal Care, and were reviewed and approved by UBC. PTPα-null mice (Ponniah et al. 1999) were backcrossed with C57BL/6 mice for 10 generations. Heterozygous PTPα$^{+/-}$ C57/BL6 mice were bred to generate PTPα$^{+/+}$, PTPα$^{+/-}$, and PTPα$^{-/-}$ offspring. Homozygous breeding of PTPα$^{+/+}$ or PTPα$^{-/-}$ mice produced pups of a specific genotype as sources for various culture models.

Primary Mouse Neural Stem Cell-Derived OPC Cultures Neural stem cell (NSC)-derived OPCs were prepared as described (Chen et al. 2007; Pedraza et al. 2008) with some modifications. Cell suspensions from cerebral cortices of embryonic E14.5 to E17.5 mouse embryos were filtered through a 40-μm cell strainer and plated at 1×10^6 cells per vented T_{25} flask (Corning) in neural culture medium [DMEM/F12 (Hyclone), 1× B27, 1 mM L-glutamax, 1 mM sodium pyruvate (all from Life Technologies)] supplemented with 20 ng/ml of basic fibroblast growth factor (bFGF, Peprotech), and 20 ng/ml of epidermal growth factor (EGF, Peprotech). After 3–4 days, floating neurospheres were passaged by dissociating the spheres with Accutase (Life Technologies) and the cells were seeded at 0.5×10^6 cells per flask in EGF/bFGF-containing neural culture medium. To obtain OPCs, passages 2–5 neurospheres were enzymatically dissociated with Accutase and resuspended in OPC proliferation medium [neural culture medium supplemented with 20 ng/ml of platelet-derived growth factor-AA (PDGF-AA, Peprotech) and 20 ng/ml of bFGF] to induce oligosphere formation. Oligospheres were passaged at a 1:2 ratio every 4–6 days as per procedures described previously.

To obtain OPCs for experimentation, oligospheres (passages 1–4) were dissociated with Accutase. Flow cytometry analysis showed that equivalent populations of over 80% of the dissociated WT and KO OPCs were A2B5$^+$NG2$^+$ (84% WT, 82% KO) (Online Resource Suppl. Fig. S1). For differentiation experiments, OPCs were seeded on poly-D-lysine (Sigma-Aldrich) and laminin-2 (10 μg/ml Lm2, Millipore)-coated chamber slides or dishes at $4–5 \times 10^4$ cells/cm^2 in the OPC proliferation medium. The dissociated OPCs were maintained in OPC proliferation medium for 5 days and then were cultured in differentiation medium (neural culture medium containing 10 ng/ml ciliary neurotrophic factor (CNTF, Peprotech), 5 μg/ml *N*-acetyl-L-cysteine, and 50 nM triiodothyronine) for 3 or 5 days. Immunostaining revealed that 5-day differentiated WT and KO cultures contained equivalent populations of GFAP-positive astrocytes (~22% of the DAPI-stained cells) comparable to the 25% GFAP+ population reported by others in similar cultures of neural stem cell-derived OPCs (Sharifi et al. 2013), equivalent populations of MAP2-

positive neurons (~20% of the DAPI-stained cells) and equal numbers of Sox10-positive OL lineage cells in WT and KO cultures (Online Resource Suppl. Fig. S1, and "Results").

Morphological complexity was assessed as a measure of differentiation by determining the number of processes extending from the cell body and binning each cell into one of the following groupings: simple, <5 processes; intermediate, 5–10 processes; complex, membranous web of processes that cannot be individually distinguished.

To assess Wnt activity, the TOPflash TK-luciferase reporter plasmid (Upstate Biotechnology) was introduced to dissociated neural stem cells using the Amaxa neuron nucleofection kit following the manufacturer's instructions (Lonza). The cells were plated on Lm-2/PDL-coated wells and maintained in neural culture medium for 24 h, and then in OPC proliferation medium for 2 days prior to treatment with Wnt3a (100 ng/ml, Peprotech) and/or XAV939 (0.05 μM, Tocris) for 24 h. The luminescent signal in cell lysates was measured using a plate reader.

OPC/Dorsal Root Ganglion Neuron Co-Cultures Dorsal root ganglion neurons (DRGNs) were isolated from P5–P8 pups. Briefly, the spinal column was dissected and the dorsal root ganglia were extracted into Hank's buffered saline solution (Life Technologies) and dissociated with papain (Worthington Biochemical) followed by Collagenase A (Roche). Enzymatic digestions were carried out at 37 °C for 10 min. Dissociated cells were seeded onto Lm2-coated (10 μg/ml) chamber slides in neural culture medium supplemented with 0.5% FBS and cultured at 8.5% CO_2. For the first 7 days in vitro (DIV), 10 μM 5-fluoro-2′-deoxyuridine (FUdR, Sigma) was added to the DRGN culture media to eliminate proliferating, non-neuronal cells. The DRGNs were then maintained in neural culture medium with 0.5% FBS, 49.5 μg/ml holo-transferrin, 5 μg/ml bovine insulin, 400 ng/ml L-thyroxine, and OL supplement (co-culture medium) as previously described (O'Meara et al. 2011) for another 7 days. Mouse primary OPCs were introduced to the DRGNs at a 1:1 ratio and were maintained in co-culture medium for 14 or 21 days.

Ex Vivo Cerebellar Slice Cultures Organotypic cerebellar slice cultures were established and maintained essentially as described (Hurtado de Mendoza et al. 2011). Brains of newborn mice (P1–P2) were removed and placed in ice-cold artificial cerebral spinal fluid (1 mM calcium chloride, 10 mM glucose, 4 mM potassium chloride, 5 mM magnesium chloride, 26 mM sodium bicarbonate, 246 mM sucrose). Excess brain tissue was removed, leaving the cerebellum attached to the underlying piece of hindbrain, and this was embedded in 4% agar. Using a vibratome, 400-μm sagittal slices of the cerebellum were sectioned. The cerebellum was teased apart from the attached hindbrain in the slices using a pair of 21-gauge needles. The cerebellar slices were placed on Millicell-CM organotypic culture inserts (Millipore) in slice culture medium containing 25% heat-inactivated horse serum, glutamax, penicillin-streptomycin (each from Invitrogen), and glucose (Sigma) in minimum essential medium. For drug treatment, DMSO or XAV939 (EMD Biosciences) was added at the time of plating. Cultures were maintained at 37 °C, and 5% CO_2 and medium was replaced every 2 days.

Immunohistochemistry, Fluorescent Microscopy, and Signal Quantification Primary OPCs and OPC/DRGN co-cultures were washed once with ice-cold PBS and fixed in 4% paraformaldehyde for 15 min. The cells were washed with PBS and permeabilized with 0.2% PBS-Triton X-100 (PBS-Tx) for 15 min and blocked in 10% normal goat serum for 1 h at room temperature. Primary antibodies (mouse anti-CNPase, 1:500, Sigma; rat anti-MBP, 1:500, Chemicon; rabbit [Millipore] or mouse [R&D Systems] anti-Sox10, 1:500; rabbit anti-NG2, 1:500, Chemicon; chicken anti-neurofilament 200 (NFH), 1:500, Aves Labs; mouse anti-TCF4, 1:500, clone 6H5–3 from Millipore) were diluted in blocking solution and incubated at 4 °C overnight followed by three washes in PBS-Tx and incubation with the appropriate fluorophore-conjugated secondary antibodies.

Cerebellar slices were washed once with ice-cold PBS, immersed in 4% paraformaldehyde for 30 min, rinsed twice with PBS, permeabilized with 0.2% Triton X-100 (*w*/*v*) in PBS, and blocked in 10% normal goat serum for 2 h at room temperature. Primary antibodies (rat anti-MBP, 1:500, Chemicon; chicken anti-NFH, 1:500, Aves Labs; and rabbit anti-CASPR, 1:500, Abcam) were diluted in blocking solution and were incubated with the slices at 4 °C with shaking.

MBP and NFH signal quantification in co-cultures and slice cultures was performed essentially as described (Zhang et al. 2011). Confocal z-stack images were acquired at 0.5-μm intervals at ×20 magnification. Thresholding was applied automatically using ImageJ. Compressed images were used to create a binary mask for NFH signal, and the percentage of the field area that was immunopositive for NFH was measured using ImageJ (% NFH, indicating density of the neurite bed). Similarly, a binary mask was also created for MBP and the percentage of the field area that was positive was measured (% MBP). A binary mask of MBP/NFH co-positivity was generated and extracted using the co-localization plug-in in ImageJ. Myelin formation was quantified by dividing the MBP+/NFH+ area by the NFH-positive area and multiplying by 100 to determine the percentage of the neurite bed that co-localized with MBP. To measure the length of MBP/NFH co-localized segments in co-cultures, binary masks representing MBP/NFH co-localized signal were extracted. The segments were traced using the NeuronJ plug-in in ImageJ, and the length per segment and segment numbers calculated using the software.

Immunoblotting Cells were washed twice with ice-cold PBS and lysed in RIPA buffer (50 mM Tris-HCL pH 7.4, 150 mM NaCl, 0.5% sodium deoxycholate, 1% Nonidet P-40, 0.1% SDS, 1 mM EDTA, 2 mM sodium orthovanadate, 50 mM sodium fluoride, 10 μg/ml of aprotinin, 10 μg/ml of leupeptin, and 1 mM phenylmethylsulfonyl fluoride). Cell lysates were incubated for 30 min on ice, and centrifuged at 12,000×*g* for 10 min at 4 °C. Equal amounts of protein were resolved by SDS-PAGE and transferred to a polyvinylidene difluoride membrane, probed with various antibodies as specified, and scanned with a LI-COR Biosciences fluorescent scanner.

Electron Microscopy Electron microscopy was performed at the UBC Centre of Heart Lung Innovation at St. Paul's Hospital. OL/DRGN co-cultures (Permanox dish, 6 mm × 6 mm well) were fixed in 2.5% glutaraldehyde in 0.1 M sodium cacodylate buffer for 30 min, washed 3 × 15 min in 0.1 M sodium cacodylate buffer, post fixed in 1% osmium tetroxide in cacodylate buffer for 45 min, washed in 0.1 M acetate buffer (pH 4.5) for 2 × 10 min, and then incubated in 2% aqueous uranyl acetate for 30 min. This was followed by dehydration in a graded series of alcohol (15 min each) and then infiltration and embedding in Epon. Cured blocks of samples were sawed out, and 60-nm thin sections were cut either en face or at cross section of the cells. Sections were contrast stained with 2% uranyl acetate and Sato's Lead and imaged on a Tecnai 12 Transmission Electron Microscope.

Statistical Analyses Data from experiments were analyzed as follows: two-way ANOVA followed by post hoc analysis (cerebellar slice cultures), Student's *t* test (OPC cultures), and Student's *t* test or one- or two-way ANOVA followed by post hoc analysis (OPC/DRGN co-cultures). Differences with a P value <0.05 were considered significant. All analyses were performed using the Prism software (GraphPad).

Results

PTPα Promotes Myelination in Cerebellar Slice Cultures

To investigate the role of PTPα in myelination, we established a model of developmental myelination using organotypic cultures of cerebellar slices (Hill et al. 2014; Hurtado de Mendoza et al. 2011; Zhang et al. 2011) from PTPα WT and KO P1-P2 mice. Slices were cultured for 10 or 20 DIV and immunostained for MBP and NFH or CASPR (Fig. 1a–f). At 10 DIV, MBP expression was visually lower and the percentage of MBP (positive area per field) was significantly reduced in KO slices compared to WT slices (Fig. 1b, g). By 20 DIV, MBP expression and the percentage of MBP in KO slices had increased to levels similar to those in WT slices (Fig. 1e, g), suggesting that OPC differentiation is delayed in the absence of PTPα but not permanently impaired. The similar percentage of NFH signals in KO and WT slices at both times (Fig. 1h) indicates that an equivalent neuron density is established, independent of PTPα, to support myelination. At 10 DIV culture, myelin formation was greatly impaired in KO slices compared to WT slices (16.5 ± 7.7 vs. 6.1 ± 6.4%) (Fig. 1i). Despite the apparent recovery in MBP expression and/or elaboration of MBP+ cell processes in KO OPCs at 20 DIV (% MBP, Fig. 1g), myelin segment formation was still reduced (21.9 ± 11.5 vs. 9.0 ± 4.9%) (Fig. 1i) with little indication of any time-dependent improvement relative to WT cultures (KO lower than WT by 2.7-fold at 10 DIV, and 2.4-fold at 20 DIV). As a measure of functional myelination, we determined the formation of nodes of Ranvier by visualizing flanking CASPR-positive paranodes (Fig. 1b, c, e, f). Node formation increased ~3-fold from 10 to 20 DIV in WT and KO slices, but was significantly and consistently reduced at both times in the KO compared to the WT slices (5.0 ± 3.3 in WT vs. 1.0 ± 0.9 in KO at 10 DIV; 14.0 ± 2.8 in WT vs. 3.0 ± 2.77 in KO at 20 DIV) (Fig. 3j). The prolonged defects in myelin segment and node formation in KO slices indicate that PTPα plays a critical role in myelination, with its absence either severely delaying or ultimately limiting myelination. We proceeded to optimize and establish other model systems to identify the specific role(s) of PTPα in this process.

Impaired Differentiation of PTPα-Deficient OPCs in Optimized in Vitro Cultures

We optimized culture conditions to promote the survival of differentiating NSC-derived primary WT and PTPα-null (KO) mouse OPCs from 2 days (Wang et al. 2009) to 5–7 days (see "Materials and Methods") by extending the proliferation time prior to inducing differentiation, including CNTF in the differentiation medium, and culturing the OPCs on laminin-2 (Lm2). After 5 days differentiation on Lm2, more WT cells expressed the mature oligodendrocyte marker MBP than did KO cells and fewer cells in WT cultures expressed the progenitor marker NG2 compared to KO cultures (Fig. 2a) despite equivalent pre-differentiation WT and KO populations of >80% $A2B5^{+}NG2^{+}$ OPCs (Online Resource Suppl. Fig. S1). At 5 days, the MBP+/Sox10+ cell ratio in the WT cultures was more than double that in the KO cultures (Fig. 2b) with the number of Sox10+ cells remaining relatively similar between all cultures from 3 to 5 days (Fig. 2c). MBP expression and that of CNPase, another protein that is increasingly expressed upon OL differentiation, were reduced in lysates of differentiating KO cells, and at 5 days were about 40% lower in the KO compared to the WT cultures (Fig. 2d, e). After 5 days differentiation, more WT than KO OPCs exhibited complex morphological elaboration of cell processes, with about 70% of the WT cells

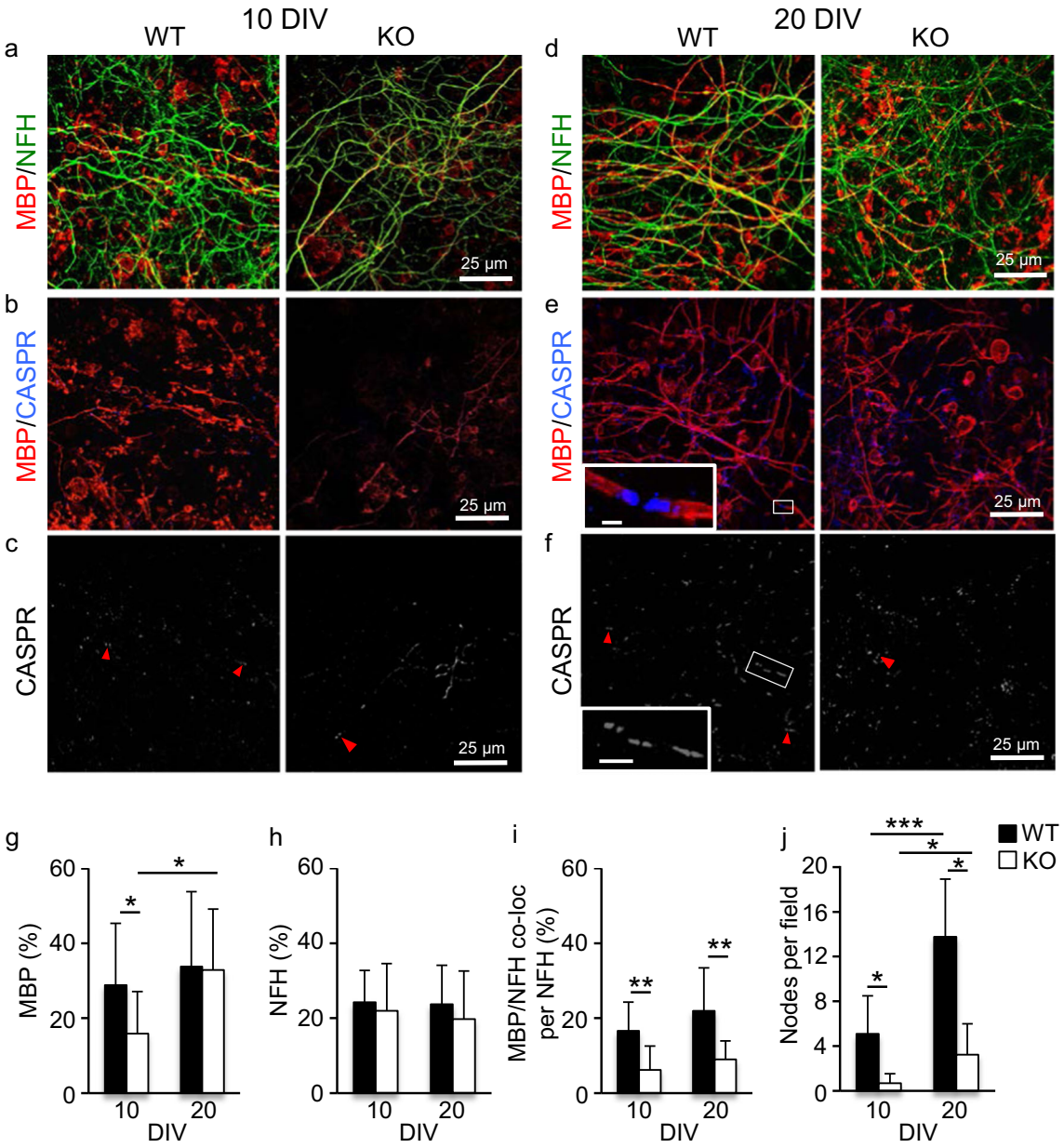

Fig. 1 PTPα regulates developmental myelination in ex vivo cerebellar slice cultures. Cerebellar slices from P1–P2 WT or KO mouse pups were maintained for 10 or 20 days in vitro (DIV) and co-stained for MBP (myelin, *red*) and NFH (axons, *green*) or CASPR (paranodes, *blue*). Representative images of MBP/NFH co-localization and MBP/CASPR staining in WT and KO cerebellar slices at (**a**–**c**) 10 DIV and (**d**–**f**) 20 DIV. In (**e**) (*left*), the *inset* is a magnified view of the area within the *white square*, *scale bar* = 3 μm, showing the molecular organization of the node (*empty space*) flanked by a pair of paranodes and internode that indicates functional myelination. The *bottom panels* in (**c**) and (**f**) are replicates of those in (**b**) and (**e**), respectively, and show only CASPR staining in *white*. *Arrowheads* indicate some CASPR-positive paranodes. In (**f**) (*left*), the *inset* is a magnified view of the area within the *white square*, *scale bar* = 5 μm, showing the paranodal organization of CASPR positivity. (**g**) The percentage of MBP signal per visual field was measured. (**h**) Axon density was determined by measuring the percentage of NFH signal per visual field. (**i**) Quantification of myelination using the ratio of co-localized MBP and NFH signal over total NFH per field. (**j**) The number of CASPR/MBP organized domains surrounding nodes was counted per field. Data in (**g**–**j**) are shown as mean ± SD quantified in 9–11 slices (obtained from at least 9 animals) per timepoint. A total of 20 slices from 16 WT pups and 19 slices from 17 KO pups were used. $^{*}P < 0.05$, $^{**}P < 0.01$, $^{***}P < 0.001$, two-way ANOVA followed by Bonferroni's post hoc test

having intermediate and complex phenotypes compared to only about 33% of the KO OPCs (Fig. 2f). Taken together, this confirms that PTPα positively regulates the differentiation and maturation of OLs and extends this to Lm2-stimulated differentiation.

Glial and Neuronal PTPα Promote Myelination in OPC/DRGN Co-Cultures

Since PTPα is ubiquitously expressed, we investigated the roles of oligodendroglial and neuronal PTPα in myelin

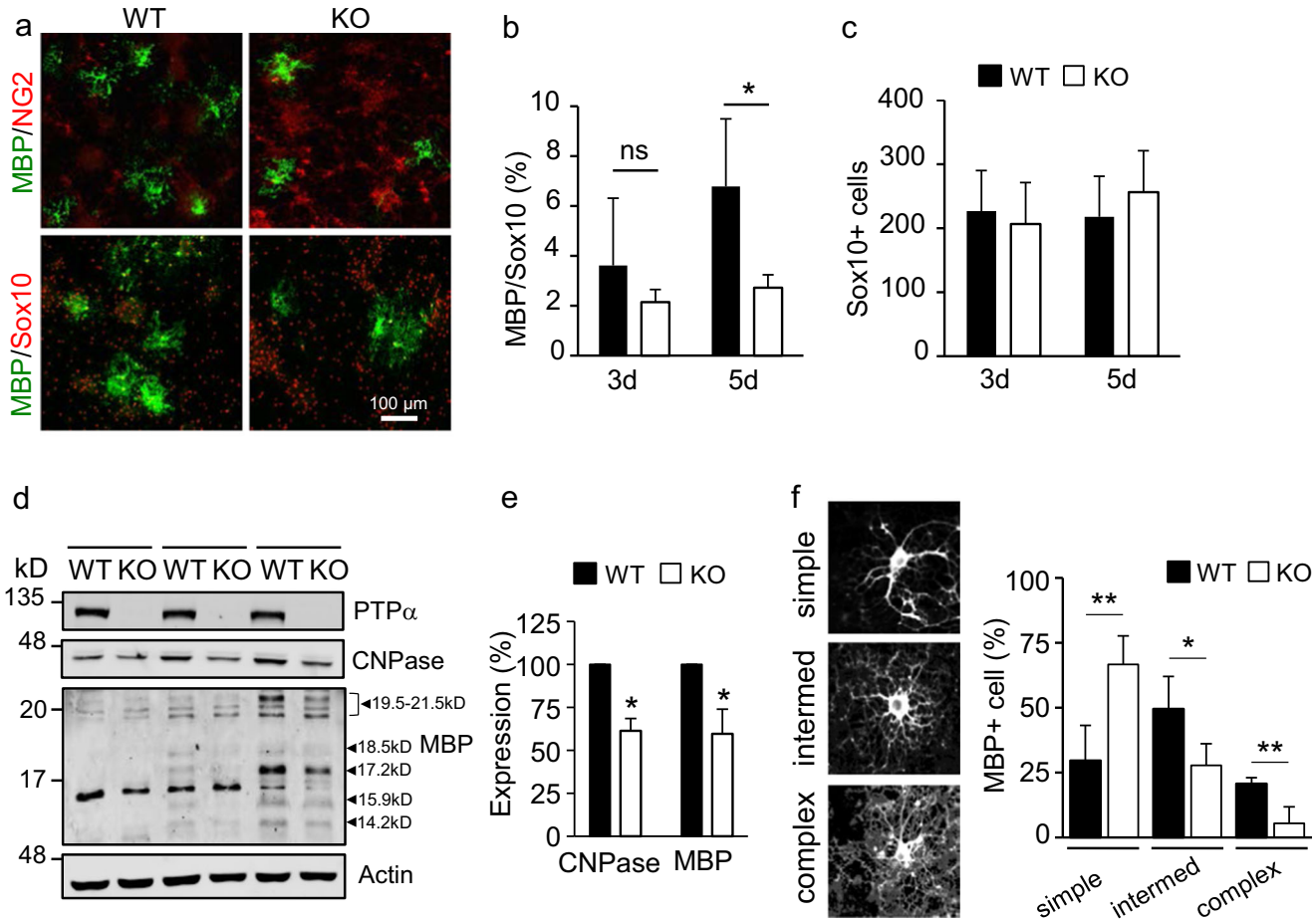

Fig. 2 Differentiation of primary mouse OPCs is impaired in the absence of PTPα. WT and KO OPCs were seeded onto PDL and Lm2-coated chamber slides and allowed to proliferate for 5 days, followed by 3–5 days of differentiation. **a** After 5 days differentiation, cells were co-stained for markers of OPCs (NG2), mature OLs (MBP), and OL lineage cells (Sox10). *Images* are representative of those obtained in at least three independent experiments. **b**, **c** Quantification of the percentage of MBP-expressing Sox10-positive cells at 3 and 5 days differentiation. The MBP/Sox10 double-positive and Sox10-positive cells were counted in six–eight areas that were randomly imaged in each of the three independent experiments. **d** Immunoblot analysis of the expression of mature OL markers CNPase and MBP in undifferentiated OPCs and OPCs that were differentiated for 3 and 5 days. The *arrowheads* indicate bands corresponding to known MBP mouse isoforms of 14–21 kD, selected based on no to low detectable levels at day 0. **e** The MBP, CNPase, and actin signals after 5-day differentiation were quantified by densitometry from blots from three independent experiments as in (**d**) The sum densitometric signal of the MBP isoforms indicated by the *arrowheads* was used to determine the total MBP expression. The MBP/actin and the CNPase/actin ratios were calculated, and those from WT cells were taken as 100% with the expression in KO cells shown relative to that. **f** The morphologies of MBP+ cells were characterized in terms of complexity as depicted by the *pictures* on the *left* and counted. The WT and KO cell populations with simple, intermediate (intermed), and complex morphologies are shown in the *graph*. At least 150 cells were counted per genotype. The *bars* in all *graphs* show the mean ± SD, $n = 3$. $^{*}P < 0.05$, $^{**}P < 0.01$, unpaired Student's t test

formation using co-cultures of mouse primary OPCs and dorsal root ganglion neurons (DRGNs) on Lm2 substrate, employing different combinations of these cell types from WT and KO mice (Fig. 3a–l). To determine glial-specific actions of PTPα, WT or KO OPCs were cultured on WT DRGNs, and neuronal actions of PTPα were investigated by co-culturing WT OPCs with WT or KO DRGNs. After 14 days, co-cultures were immunostained for MBP and NFH and these signals quantified (Fig. 3n, o). The equivalent percentage of NFH signal in parallel cultures indicated that neuronal beds of similar densities were formed by the DRGNs irrespective of DRGN or OPC genotype. Myelin formation was assessed by quantifying the co-localized MBP and NFH signals in binary images (Fig. 3c, f, i, l) and dividing by the total NFH signal per field (Fig. 3p). As discussed (Kerman et al. 2015), this cannot identify or distinguish between axon ensheathment and compact myelin formation, although both are potentially present/in progress as electron microscopy confirmed that compact myelin had formed in the 4-week WT OPC/DRGN cultures (Fig. 3m).

Oligodendroglial PTPα promoted myelin formation, since this was significantly reduced by about 50% in 14-day KO OPC/WT DRGN co-cultures compared to WT OPC/WT DRGN co-cultures (8.42 ± 1.57% with KO OPCs vs.

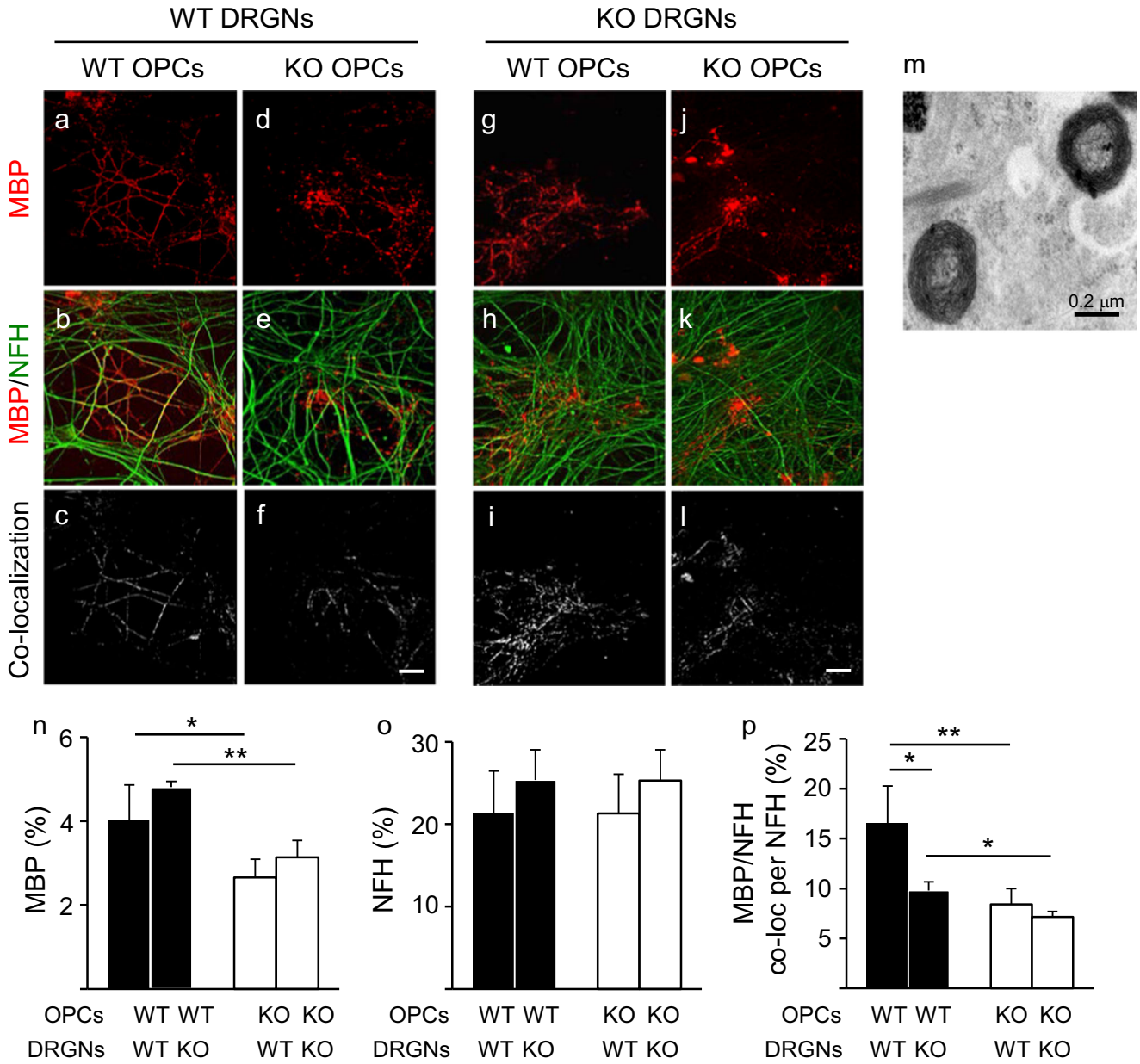

Fig. 3 Oligodendroglial and neuronal PTPα promote myelination in OPC/DRGN co-cultures. **a**–**l** WT or KO primary OPCs were co-cultured with WT or KO DRGNs as shown for 14 days and co-stained for NFH (neurons, *green*) and MBP (oligodendrocytes, *red*). Merged images (**b**, **e**, **h**, **k**) and binary masks of co-localized MBP and NFH signals (**c**, **f**, **i**, **l**) are shown. *Scale bars* = 25 µm. **m** A 28-day WT OPC/DRGN co-culture was visualized using electron microscopy. **n** The percentage of MBP positivity per visual field in 14-day co-cultures was measured. **o** Neurite bed density was determined by measuring the percentage of NFH signal per visual field. **p** The co-localization of MBP/NFH co-staining per NFH signal was determined. The quantified data in (**n**–**p**) were from 10 fields per experiment and three independent experiments. All *graphs* show the mean ± SD, and *asterisks* show significant differences (unpaired Student's *t* test, $*P < 0.05$, $**P < 0.01$)

16.83 ± 3.48% with WT OPCs, $P < 0.01$, $n = 3$) (Fig. 3p). This correlated with the reduced percentage of MBP signal in the KO OPC containing co-cultures (Fig. 3n) that could reflect impaired MBP expression or morphological elaboration of maturing OLs. After 21 days in culture, similar impairments in percentage of MBP signal and myelin formation were detected in the KO OPC/WT DRGN co-cultures (MBP/NFH co-localization per NFH: 9.00 ± 1.48% with KO OPCs vs. 19.14 ± 2.31% with WT OPCs, $P < 0.01$, $n = 3$) (data not shown). Since myelin formation was not greatly altered from the respective 14-day cultures, all subsequent measurements were conducted on 14-day co-cultures. Visually, the myelin represented by co-localized MBP/NFH signals in WT OPC/WT DRGN co-cultures appeared as organized linear tracts expected of myelinated segments, but this was less obvious in the KO OPC/WT DRGN co-cultures (compare Fig. 3c and f).

A distinct but similarly impactful role of neuronal PTPα was evident from the reduced myelin formation indicated by

reduced MBP/NFH co-localization when WT OPCs were co-cultured with KO DRGNs compared to WT DRGNs (9.81 ± 0.85% with KO DRGNs vs. 16.83 ± 3.48% with WT DRGNs, $P < 0.05$, $n = 3$) (Fig. 3p). Interestingly, despite this reduced MBP/NFH co-localization in the WT OPC/KO DRGN co-cultures, equivalent percentage of MBP signals and equivalent percentage of NFH signals were measured in the co-cultures of WT OPCs with WT or KO DRGNs (Fig. 3n, o), suggesting that the KO DRGNs are less efficient in developing or sustaining axo-glial interactions to promote myelinating events. There was no detectable effect of neuronal PTPα in regulating MBP/NFH co-localization in KO OPC co-cultures (Fig. 3p, compare KO OPCs cultured with WT vs. KO DRGNs), likely because the extent of co-localization was already minimal due to the deleterious effects of oligodendroglial PTPα ablation.

Suppressing Wnt Signaling Improves OPC Differentiation in a PTPα-Independent Manner

A complexity of extrinsic and intrinsic OL signaling pathways positively and negatively regulates differentiation and myelinating ability, but signal integration and coordination remain poorly understood. PTPα signaling promotes OPC differentiation by activating the Src family tyrosine kinase Fyn and regulating Fyn-dependent activation of FAK, Rac1, and Cdc42 while inhibiting Rho (Wang et al. 2009), but little else is known of other PTPα signaling or its regulation in oligodendrocytes. Having characterized oligodendroglial PTPα-dependent defects in differentiation and myelin formation, we wished to investigate if these could be ameliorated by targeted signaling interventions, with the potential to identify PTPα interacting or independent signaling pathways.

In initial tests of the ability of various signaling inhibitors/activators to improve PTPα-KO OPC differentiation, we found that this was enhanced by the Wnt/β-catenin signaling inhibitor XAV939. Canonical Wnt/β-catenin signaling negatively regulates OPC differentiation, although it plays controversial roles in multiple aspects of OL development and myelination that are likely modulated through cross talk with other signaling pathways (Guo et al. 2015; Xie et al. 2014). There are no reports of integrated PTPα and Wnt signaling, but PTPα effector molecules such as SFKs, FAK, and Rho can impact Wnt/β-catenin signaling in OLs and other cell types (Imada et al. 2016; Lee et al. 2015; Rossol-Allison et al. 2009; Williams et al. 2015). We thus used the various model systems described previously to investigate if inhibiting Wnt signaling could overcome PTPα-dependent defects in OL differentiation and myelin formation, and if so, whether this represented independent or intersecting signaling effects.

The Wnt signaling inhibitor XAV939 is a small molecule tankyrase inhibitor that acts to stabilize Axin2 to promote β-catenin degradation (Fancy et al. 2011; Huang et al. 2009). We confirmed that XAV939 stabilized Axin expression (Fig. 4a) and blocked Wnt3a-induced luciferase activity in OPC cultures expressing the TOPflash Wnt activity reporter plasmid (Fig. 4b). In differentiating OPC cultures, XAV939 treatment restored KO OPC differentiation to a level similar to vehicle-treated WT OPCs (Fig. 4c, d). It also induced similar fold increases in differentiated MBP/Sox10-expressing WT OPCs, although the differentiation of XAV939-treated KO OPCs was consistently ~2-fold lower (Fig. 4d). This suggested that PTPα might promote differentiation in a manner distinct from that of suppressing Wnt signaling, and we therefore determined if Wnt signaling was altered in OPCs lacking PTPα by quantifying the expression of the Wnt target TCF4 (Fig. 4e, f). This was significantly reduced in differentiating WT and KO OPCs compared to proliferating cells, and was unaffected by the presence or absence of PTPα. Concomitant with promoting OPC differentiation, XAV939 further repressed Wnt signaling in differentiating WT and KO OPCs and did so to the same extent in both cell types (Fig. 4e, f). Total Sox10+ cell numbers were not significantly different between WT and KO cultures under all conditions shown in Fig. 4e, f (data not shown). Altogether, these results indicate that Wnt signaling in OPCs is PTPα-independent, and that while inhibiting Wnt signaling cannot compensate for the absence of PTPα, it improves the differentiation of KO OPCs.

Fig. 4 XAV939 inhibits Wnt signaling and promotes differentiation of WT and KO OPCs. **a** Differentiating WT and KO OPCs were treated with 0.05 μM of XAV939, and lysates were probed for PTPα, Axin, and actin. **b** WT OPCs expressing TOPflash Wnt reporter plasmid were treated with Wnt3a (100 ng/ml), XAV939 (0.05 μM), or both for 24 h, and luciferase activity was measured. The *graph* shows the average of two independent experiments, and the *bars* on each column show the range of the two values. **c**, **d** WT and KO OPCs were cultured in differentiation conditions for 5 days in the absence or presence of 0.05 μM XAV939 and (**c**) immunostained for MBP and Sox10. **d** The number of MBP-positive and Sox10-positive cells were counted in six–eight areas randomly chosen from images of an experiment as in (**c**), and the *graph* shows the percentage of double-positive cells as the mean ± SD from three independent experiments. Two-way ANOVA followed by Bonferroni's post hoc test, $*P < 0.05$. **e**, **f** WT and KO OPCs were cultured in proliferating conditions for 5 days, and subsequently fixed or differentiated for 5 days in the absence or presence of 0.05 μM XAV939 and (**e**) immunostained for TCF4 and Sox10. **f** TCF4+/Sox10+ cells were counted in six–eight areas randomly chosen from *images* from each of three independent experiments as in (**a**). The *bars* depict the numbers of TCF4+/Sox10+ cells as mean ± SD relative to those in untreated proliferating WT OPC cultures that were taken as 100%. One-way ANOVA followed by Tukey's post hoc test, $*P < 0.05$, $**P < 0.01$, $\#P < 0.001$

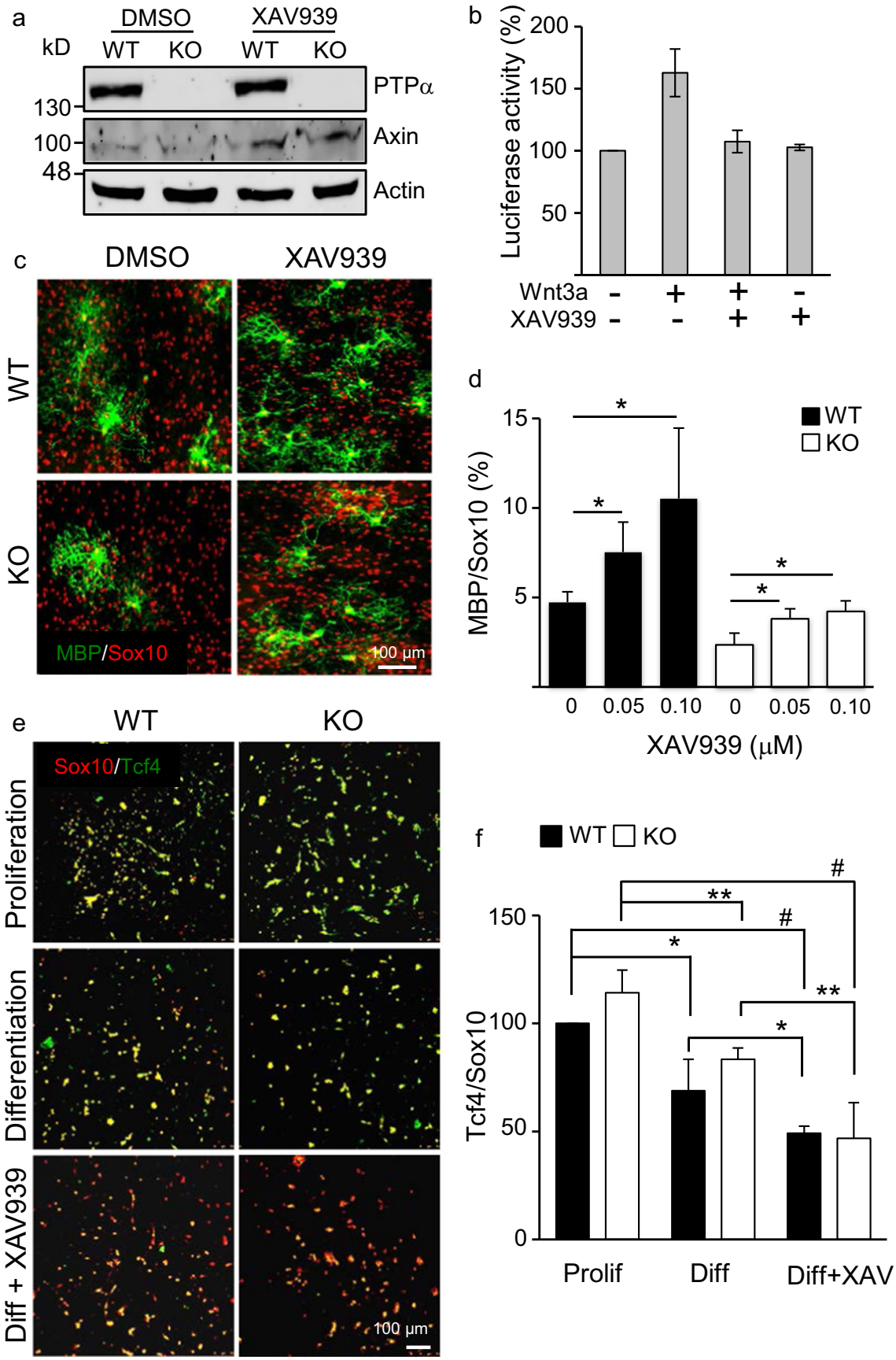
a
DMSO
XAV939
kD
WT
KO
WT
KO
130
100
48
PTPα
Axin
Actin
b
Luciferase activity (%)
200
150
100
50
Wnt3a - + + -
XAV939 - - + +
c
DMSO
XAV939
WT
KO
MBP/Sox10
100 μm
d
MBP/Sox10 (%)
15
10
5
WT
KO
*
*
*
*
0 0.05 0.10 0 0.05 0.10
XAV939 (μM)
e
WT
KO
Sox10/Tcf4
Proliferation
Differentiation
Diff + XAV939
100 μm
f
WT KO
Tcf4/Sox10
150
100
50
0
#
**
#
*
**
*
Prolif
Diff
Diff+XAV

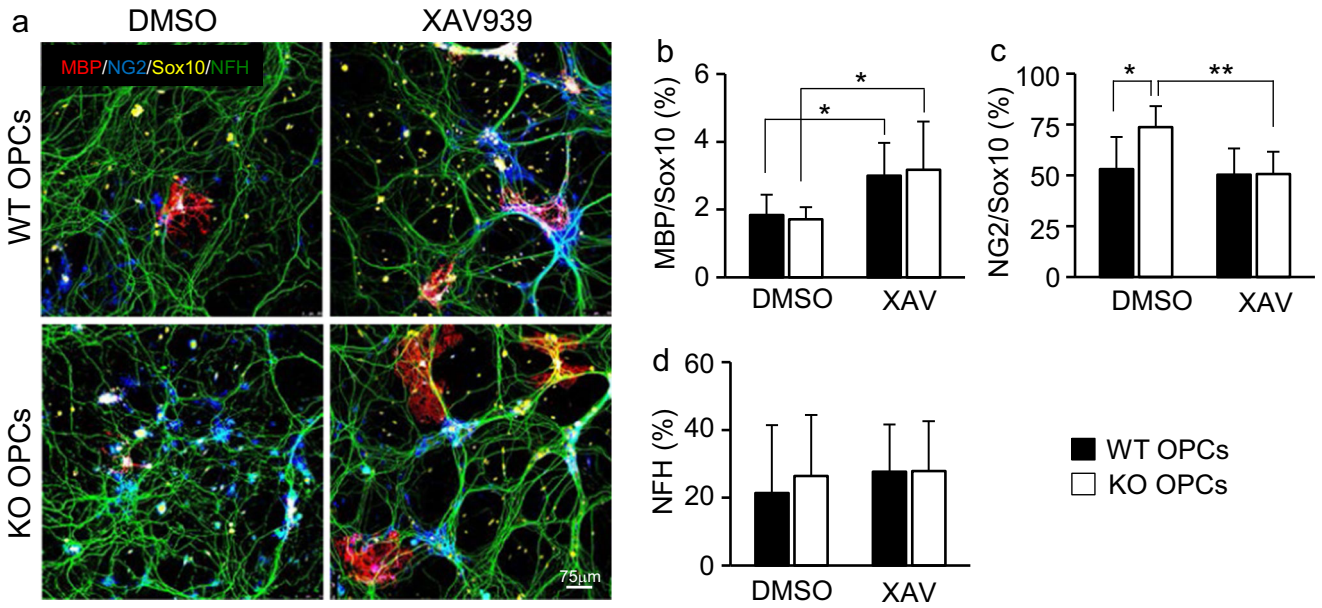

Fig. 5 XAV939 increases populations of WT and KO MBP+ OLs and decreases KO NG2+ OPCs. WT and KO OPCs were seeded on neurite beds and co-cultured for 14 days in the presence of 0.05 μM XAV939 or DMSO vehicle. (**a**) The cultures were stained for MBP (*red*), NG2 (*blue*), Sox10 (*yellow*), and NFH (*green*). *Scale bar* = 75 μm. OPC differentiation was assessed by quantifying the percentage of (**b**) MBP/Sox10 and (**c**) NG2/Sox10 cells. (**d**) Neurite beds were identified by NFH positivity and the percentage of signal per field was determined. Three–six areas with comparable neurite beds were imaged and analyzed for each of four independent experiments. The *bars* in the *graphs* show mean ± SD, and the *asterisks* show significant differences (unpaired Student's *t* test, $*P < 0.05$, $**P < 0.01$)

XAV939 Promotes Differentiation of NG2+ KO OPCs in DRGN Co-Cultures

We also investigated the effect of XAV939 on OPC differentiation in DRGN co-cultures, wherein 14-day co-cultures were immunostained for MBP, NG2, Sox10, and NFH (Fig. 5a). There were no significant differences in total Sox10+ cell numbers between WT and KO OPC co-cultures, either in the presence or the absence of XAV939 (data not shown). Interestingly, similar populations of MBP/Sox10-positive cells were present in control KO and WT OPC-containing DRGN co-cultures at 14 days (Fig. 5b), in contrast to the higher population of MBP/Sox10 cells in WT vs. KO OPCs cultured alone for 5 days (Fig. 4d), perhaps reflecting an early delay in differentiation of PTPα-null OPCs that resolves over the more extended 14-day co-culture time. XAV939 promoted equivalent increases in the MBP/Sox10-positive populations in WT and KO OPC co-cultures (Fig. 5b), while neuron density was unaffected by OPC genotype or by XAV939 (Fig. 5d). However, even after 14 days co-culture, more control-treated KO OPCs than WT OPCs were NG2/Sox10 positive. XAV939 treatment significantly reduced the population of these immature NG2/Sox10-positive KO OPCs (from 73.7 ± 10.4 to 50.6 ± 11.0%) to a level equivalent to that in the untreated and XAV939-treated WT OPC populations (53.0 ± 15.9 and 50.3 ± 12.9%, respectively) (Fig. 5c). These results show that XAV939 promotes both WT and KO OPC differentiation in co-culture, and specifically acts on NG2-positive KO progenitor cells to enhance their transition to an NG2-negative, more differentiated stage.

XAV939 Promotes the Formation of Short Myelin Segments by KO OPCs in DRGN Co-Cultures

To determine if XAV939-induced OPC differentiation resulted in enhanced myelin formation in OPC/DRGN co-cultures, we assessed MBP/NFH co-localization per percentage of NFH (Fig. 6). This was improved by XAV939 treatment of KO OPC co-cultures to levels comparable to those observed

Fig. 6 XAV939 does not remediate PTPα-dependent myelin defects in OPC/DRGN co-cultures. WT and KO OPCs were co-cultured with WT DRGNs in the presence of XAV939 or DMSO vehicle for 14 days and co-stained for MBP (*red*) and NFH (*green*). Representative *images* of MBP staining (**a**–**d**), merged NFH/MBP staining (**e**–**h**), and binary masks of co-localized MBP and NFH signals (**i**–**l**) from control DMSO-treated and 0.05 μM XAV939-treated cultures are shown. (**m**) The percentage of MBP signal positivity per visual field, and (**n**) the co-localization of MBP/NFH co-staining per NFH signal were quantified from 10 fields per experiment and three independent experiments. (**o**) The number of MBP-positive/NFH segments per visual field and (**p**) the average length of MBP-positive/NFH segments were determined from binary images of co-localized MBP/NFH signal in three fields of each of three independent 14-day co-cultures. (**q**) The size populations of MBP-positive/NFH segments in each culture condition are shown. *Graphs* show the mean ± SD, and *asterisks* show significant differences (two-way ANOVA followed by Bonferroni's post hoc tests, $*P < 0.05$, $**P < 0.01$, $***P < 0.001$)

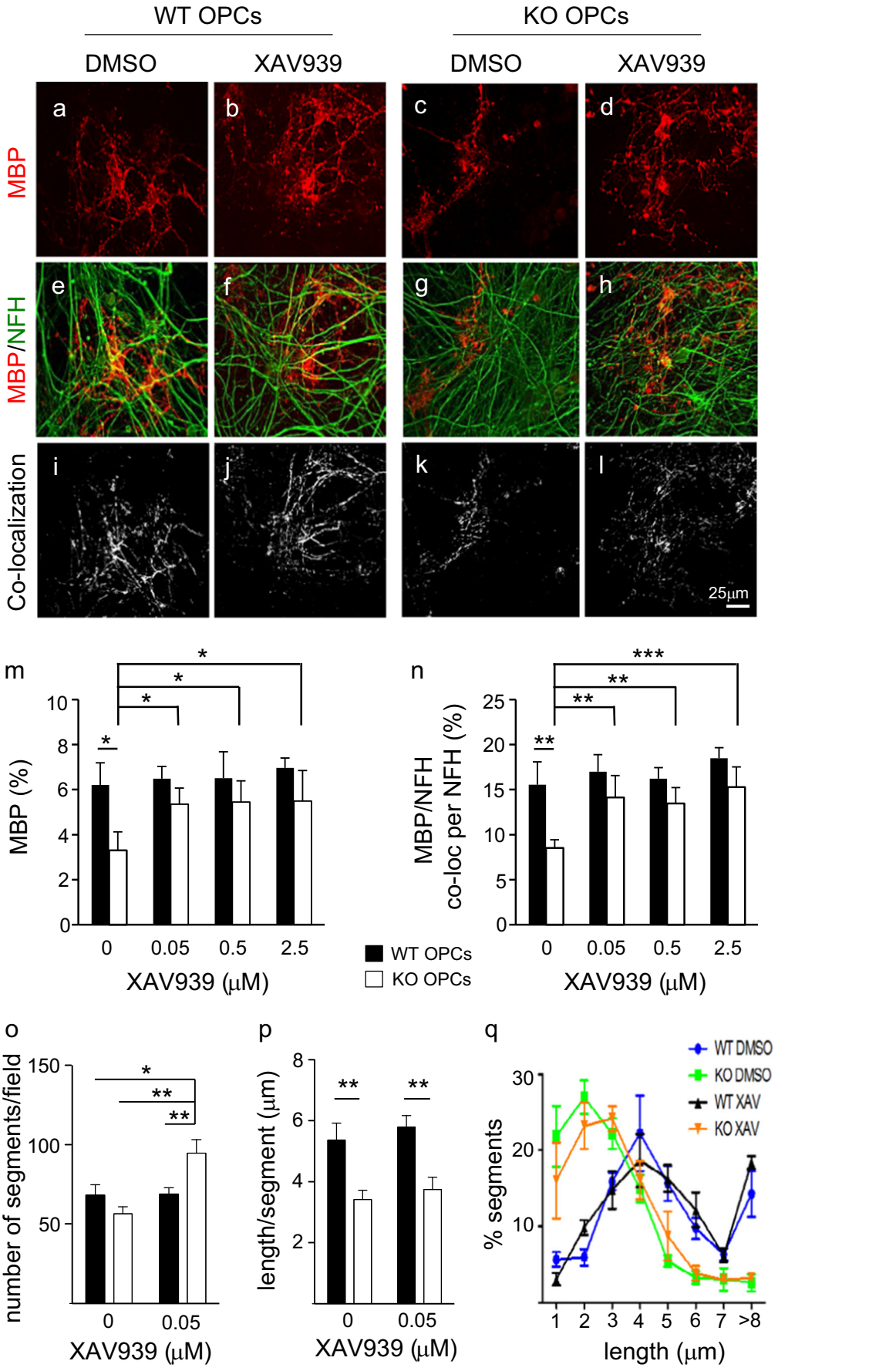
WT OPCs
KO OPCs
DMSO
XAV939
DMSO
XAV939
MBP
MBP/NFH
Co-localization
a
b
c
d
e
f
g
h
i
j
k
l
25μm
m
MBP (%)
XAV939 (μM)
0
0.05
0.5
2.5
WT OPCs
KO OPCs
n
MBP/NFH co-loc per NFH (%)
XAV939 (μM)
o
number of segments/field
XAV939 (μM)
p
length/segment (μm)
XAV939 (μM)
q
% segments
length (μm)
WT DMSO
KO DMSO
WT XAV
KO XAV

in XAV939-treated and untreated WT OPC co-cultures (Fig. 6n). Confirming that this effect of XAV939 is exerted via OPCs/OLs rather than neurons, reduced myelin formation in co-cultures of WT OPCs and KO DRGNs (Fig. 2p) was not improved by XAV939 treatment (data not shown). Interestingly, while WT and KO OPC co-cultures have equivalent populations of MBP/Sox10+ cells (Fig. 5b), the percentage of MBP (positivity/field) was significantly lower in KO OPC co-cultures (Fig. 6m). This suggests that MBP-positive KO OPCs do not spread or elaborate processes to the same extent as WT OPCs. This defect was remediated by XAV939 (Fig. 6m). Nevertheless, visual inspection of the MBP/NFH+ myelin segments suggested that WT OPC co-cultures had longer and more intensely stained areas of co-localization than were obvious in the control and XAV939-treated KO OPC co-cultures (compare Fig. 6i, j with k, l). To characterize this more precisely, the MBP/NFH co-localized segments were counted and their lengths measured. In the absence of XAV939, WT and KO OPCs formed equivalent numbers of segments (Fig. 6o), although the segments formed by WT OPCs were significantly longer than those formed by KO OPCs (Fig. 6p). Treatment with XAV939 had no effect on the number or length of the segments formed by WT OPCs, and increased the number but not the length of the segments formed by KO OPCs (Fig. 6o, p). This suggests that XAV939, in addition to or possibly because of promoting differentiation and the spreading or elaboration of KO OPCs, enhances the initial contacts formed between KO OLs and neurons but cannot rescue the impaired ability to extend myelin processes along the neurons. In support of this idea, an analysis of segment length among the populations of WT and KO OPCs co-cultured with DRGNs reveals that a majority of segments in the KO OPC co-cultures are relatively short (1–3 μm), while two distinct longer populations of segments (3–6 μm and >8 μm) are formed in the WT OPC/DRGN co-cultures, and that none of these are changed by XAV939 treatment (Fig. 6q).

XAV939 Does Not Rescue PTPα-Dependent Myelination Defects in Cerebellar Slices

Cerebellar slices from WT and KO mice (Fig. 7a–d) were treated with 0.05 μM XAV939 for 10 and 20 DIV. XAV939 significantly improved the percentage of MBP signal in KO slices at 10 DIV (from 18.2 ± 6.1 to 31.2 ± 9.1%), without significantly affecting the percentage of MBP signal in WT slices (Fig. 7e). Overall, there remained 30% less MBP-positive area in XAV939-treated KO vs. WT slices at 10 DIV. However, at 20 DIV, there was no difference in percentage of MBP positivity in control WT and KO slices, consistent with our observations in other slice cultures (Fig. 1g), and no further XAV939-mediated enhancement of MBP expression was apparent (Fig. 7i). This suggests that XAV939 may overcome an early delay in PTPα-deficient OPC maturation, but in the longer term does not affect the extent of morphological maturation achieved by MBP+ WT or KO OPCs.

Cerebellar neuron density was not affected by XAV939 or by the presence or absence of PTPα, as indicated by the unaltered NFH signal at both culture times (Fig. 7f, j). Myelin segment formation in WT and KO slices was significantly enhanced by XAV939 at 10 DIV, as evidenced by the increase in the MBP/NFH co-localization ratio by ~30% in WT and ~50% in KO cerebellar slices compared to vehicle control (Fig. 7g). By 20 DIV, this effect was no longer apparent as segment formation was similar in control and XAV939-treated slices (Fig. 7k). Furthermore, apart from an early 2-fold increase in node of Ranvier formation in XAV939-treated WT slices at 10 DIV (Fig. 7h), node formation in KO and WT slices was otherwise unaffected by this treatment and there remained significantly fewer nodes in KO slices at all times (Fig. 7h, l). Overall, XAV939 improved an early deficit in percentage of MBP signal and MBP/NFH co-localization in KO slices, but was unable to remediate PTPα-dependent defects in myelination, likely because of the neuronal PTPα deficit. XAV939 accelerated but did not enhance the intrinsic myelinating ability of WT cerebellar slices.

Discussion

PTPα-deficient mice have brain hypomyelination that is associated with impaired oligodendrocyte differentiation and maturation detected in vivo and in vitro (Wang et al. 2009, 2012). In this study, we used several complementary experimental systems involving cells and/or tissues from wild-type (WT) and PTPα knockout (KO) mice to more precisely investigate the roles of PTPα in OL differentiation and myelination. These model systems recapitulated PTPα-dependent OL differentiation/maturation defects and hypomyelination, and in conjunction with manipulated Wnt signaling, revealed specific aspects of PTPα function. We found that oligodendroglial PTPα signals independently of suppressed Wnt signaling to promote differentiation and perhaps plays another role in myelin elongation, while neuronal PTPα supports myelination.

Our study provides the first evidence that, in addition to oligodendroglial actions of PTPα that promote differentiation and myelin formation, neuronal PTPα also plays a critical role in CNS myelination. In co-cultures of OPCs and DRGNs, myelin formation was impacted to similar extents by the absence of neuronal PTPα (reduced by 42%) or oligodendroglial PTPα (reduced by 50%). The lack of neuronal PTPα did not appear to influence OPC differentiation, since WT OPCs co-cultured with WT or KO DRGNs contained equivalent areas of MBP positivity indicating similar OL morphological elaboration. Furthermore, the ablation of neuronal PTPα did not hinder neurite bed formation, nor was the presence of neuronal PTPα able to autonomously improve myelin formation in KO

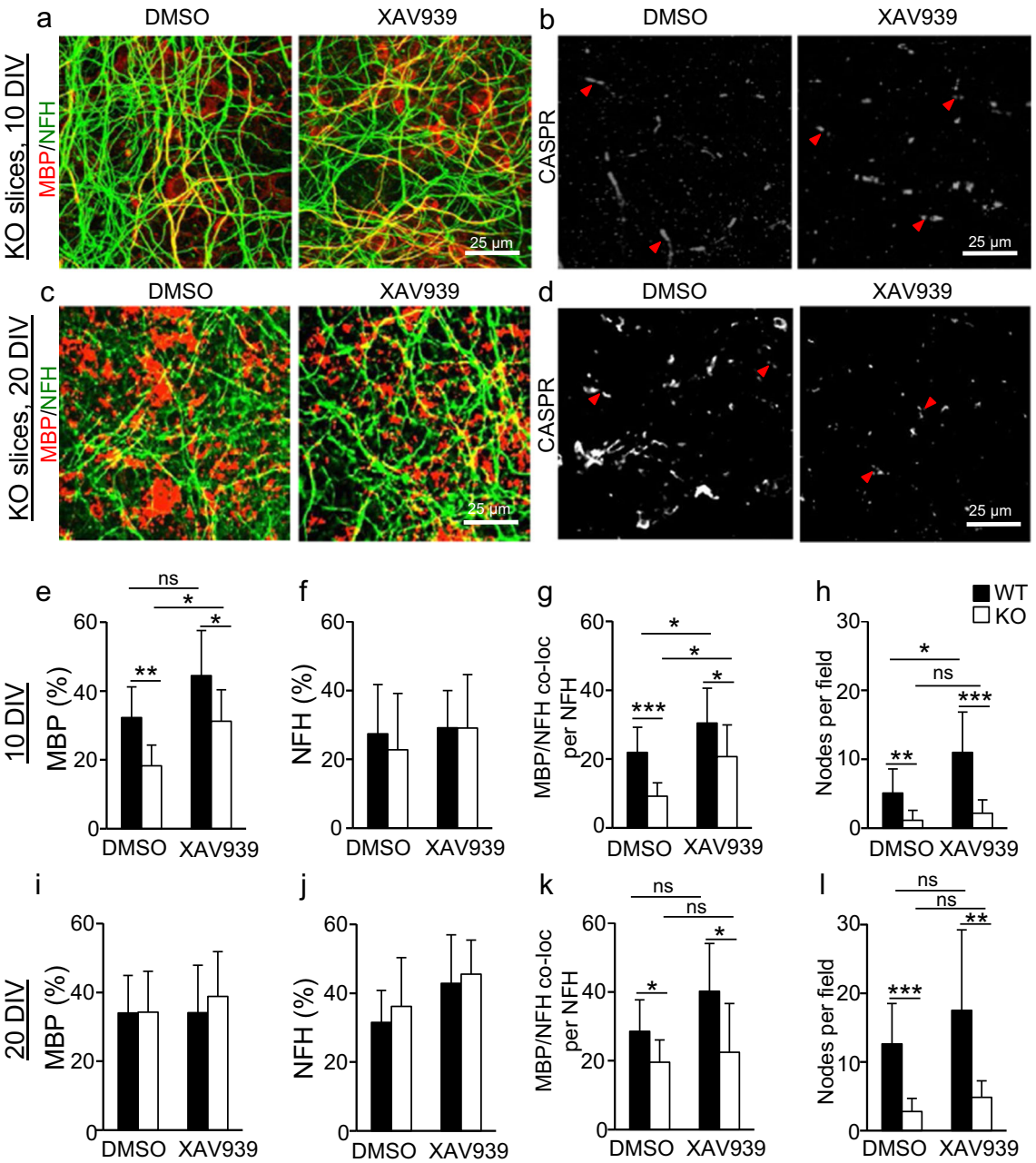

Fig. 7 XAV939 treatment does not rescue PTPα-dependent defects in myelination in cerebellar slice cultures. P1-P2 cerebellar slices from WT and KO mice were treated with 0.05 μM XAV939 or DMSO vehicle for 10 (**a**, **b**, and **e**–**h**) and 20 (**c**, **d**, and **i**–**l**) days in vitro (DIV). Slices were immunostained for MBP (OLs), NFH (axons), and CASPR (paranodes). Representative *images* of (**a**) 10 DIV and (**c**) 20 DIV KO slices treated with or without XAV939 followed by immunostaining for NFH (*green*) and MBP (*red*) co-localization. Formation of CASPR-positive paranodal structures in (**b**) 10 DIV and (**d**) 20 DIV KO slices treated with DMSO or XAV939. (**e**, **i**) The percentage of MBP signal per visual field was measured. (**f**, **j**) Axon density was determined by measuring the percentage of NFH signal per visual field. (**g**, **k**) The co-localization of MBP/NFH co-staining per NFH signal was determined. (**h**, **l**) Node formation as visualized by flanking CASPR-positive paranodes was quantified. Data in (**e**–**l**) are shown as mean ± SD quantified in 9–12 slices (obtained from at least 9 animals) per condition and timepoint. A total of 40 slices from 21 WT pups and 39 slices from 24 KO pups were used. *Asterisks* show significant differences (two-way ANOVA followed by Bonferroni's post hoc test, $*P < 0.05$, $**P < 0.01$, $***P < 0.001$)

OPC co-cultures. Altogether, this suggests that neuronal PTPα promotes myelin formation by mediating neuronal interactions with differentiated, mature OLs. We speculate that this could include the action of PTPα itself as an axonal receptor that directly engages in pro-myelinating *trans* interactions with OL receptors: the formation of PTPα complexes with neural cell adhesion molecules in *cis* [as has been reported with PTPα binding partners such as contactin or NCAM (Bodrikov et al. 2005; Zeng et al. 1999)] that productively interact with OL receptors, PTPα-regulated neuronal surface expression and

availability of OL-interacting molecules [for example, as reported with the adhesion molecule NB-3 (Ye et al. 2011)], or PTPα-mediated production of secreted neuronal factors that stimulates OL myelinating activity.

Our study also sheds new light on the oligodendroglial actions of PTPα. Previously, we observed defective differentiation of KO OPCs in 2-day cultures, as indicated by more NG2+ and fewer O4+ cells compared to WT OPC cultures. The improved conditions we instituted in this study allowed us to extend differentiating cultures to 5 days, at which time the continued presence of more NG2+ cells and the emergence of fewer and less morphologically complex MBP+ cells in KO OPC cultures showed an ongoing impairment of differentiation. Interestingly, results from longer term OPC/DRGN co-cultures suggest that this PTPα-dependent defect in differentiation of MBP-expressing OLs is a transient delay or is ameliorated by factors in the co-culture environment, as KO and WT OPCs formed equivalent populations of MBP+ OLs after 14 days co-culture with WT DRGNs. Nevertheless, the MBP+ cells in the KO OPC co-cultures generated a significantly lower area of MBP positivity (% MBP) than those in WT OPC co-cultures, indicating that morphological elaboration continued to be impaired in the absence of PTPα; and there remained an elevated population of NG2+ KO cells in the co-cultures that represent immature cells that may impede optimal myelin formation. In support of these defects being transient delays in differentiation, we noted that the reduced percentage of MBP in KO cerebellar slice cultures at 10 DIV increased to WT levels by 20 DIV, and that the population of NG2+ cells in the corpus callosum of KO mice declined between P10 and P18 to more closely approach that in the WT tissue (Wang et al. 2012). Overall, these findings suggest that oligodendroglial PTPα promotes the timely differentiation of OLs, and that retarded differentiation in the absence of PTPα can eventually be remedied through other pathways.

We used the Wnt signaling inhibitor XAV939 to try to rescue differentiation and myelination impairments in the PTPα KO model systems. The similar Wnt signaling activity, in differentiating untreated or XAV939-treated KO and WT OPCs (Fig. 5a, b), indicates that Wnt signaling is PTPα independent and not responsible for KO OPC differentiation defects. Nevertheless, additional inhibition of Wnt signaling by XAV939 improved KO OPC differentiation, significantly reducing the skewed population of NG2+ OPCs in KO OPC/DRGN co-cultures to WT levels (Fig. 5f) and increasing the populations of MBP+ OLs in differentiating WT and KO OPC cultures and DRGN co-cultures (Fig. 5d, g). The similar fold stimulation by XAV939 of MBP+ OL production from WT and KO OPCs (~1.7–1.9-fold in OPC cultures and co-cultures) also supports that this occurs independently of PTPα. Thus, PTPα-regulated signaling and suppressed Wnt signaling both positively regulate OPC differentiation but through different mechanisms.

XAV939 treatment of KO OPC co-cultures improved myelin segment formation to levels present in treated or untreated WT OPC-containing co-cultures (Fig. 6), consistent with its effects in remediating key parameters of differentiation. XAV939 also improved the defective myelin segment formation in KO cerebellar slices at 10 DIV (Fig. 7), although the impaired formation of myelinated nodes in untreated and XAV939-treated 10 and 20 DIV KO slices is likely due, at least in part, to the unremediated effects of the absence of neuronal PTPα. In KO OPC co-cultures with WT neurons, PTPα-dependent myelin formation defects were also not fully remediated by XAV939, as myelin segments remained significantly shorter than in WT co-cultures. This raises the possibility of an additional role of oligodendroglial PTPα in promoting myelin extension. While we cannot exclude that the shorter segments are due to undetected differentiation defects that may persist in the XAV939-treated KO OPC co-cultures, the observation that XAV939 increased the area of MBP positivity (% MBP) and also increased the abundance of myelin segments (to even exceed that in the WT OPC co-cultures) suggests the presence of morphologically differentiated KO OLs with plentiful neuron-contacting processes. Indeed, the presence of more short MBP/NFH+ segments may reflect attempts by XAV939/KO OLs to extend myelin processes along neurons in the face of elongation failure.

In summary, our investigation of the basis of the hypomyelination defect in PTPα-deficient mouse brain identifies PTPα as a cell-specific and stage-specific regulator of the multistep process of myelination. As a receptor-like molecule, PTPα is positioned to interact with other cell receptors in *trans* and *cis*, and to recognize and transduce extracellular signals. The molecular interactions and signaling mechanisms that mediate specific pro-myelinating actions of PTPα require further investigation.

Acknowledgements This work was supported by grants 1129 and 2366 from the Multiple Sclerosis Society of Canada (to C.J.P.). P.T.T.L is the recipient of a Postdoctoral Fellowship from the Canadian Institutes of Health Research, and C.J.P. holds an Investigator Award from the BC Children's Hospital Research Institute. We thank Dr. Chinten James Lim for valuable assistance with imaging quantification.

Compliance with Ethical Standards Animal care and use followed the guidelines of the University of British Columbia (UBC) and the Canadian Council on Animal Care, and were reviewed and approved by UBC.

References

Bercury KK, Macklin WB (2015) Dynamics and mechanisms of CNS myelination. Dev Cell 32(4):447–458

Bodrikov V, Leshchyns'ka I, Sytnyk V, Overvoorde J, den Hertog J, Schachner M (2005) RPTPalpha is essential for NCAM-mediated p59fyn activation and neurite elongation. J Cell Biol 168(1):127–139

Buttermore ED, Thaxton CL, Bhat MA (2013) Organization and maintenance of molecular domains in myelinated axons. J Neurosci Res 91(5):603–622

Chang KJ, Rasband MN (2013) Excitable domains of myelinated nerves: axon initial segments and nodes of Ranvier. Curr Top Membr 72: 159–192

Chen Y, Balasubramaniyan V, Peng J, Hurlock EC, Tallquist M, Li J, Lu QR (2007) Isolation and culture of rat and mouse oligodendrocyte precursor cells. Nat Protoc 2(5):1044–1051

Fancy SP, Harrington EP, Yuen TJ, Silbereis JC, Zhao C, Baranzini SE, Bruce CC, Otero JJ, Huang EJ, Nusse R, Franklin RJ, Rowitch DH (2011) Axin2 as regulatory and therapeutic target in newborn brain injury and remyelination. Nat Neurosci 14(8):1009–1016

Guo F, Lang J, Sohn J, Hammond E, Chang M, Pleasure D (2015) Canonical Wnt signaling in the oligodendroglial lineage-puzzles remain. Glia 63(10):1671–1693

Hill RA, Medved J, Patel KD, Nishiyama A (2014) Organotypic slice cultures to study oligodendrocyte dynamics and myelination. Journal of visualized experiments : JoVE 90:e51835

Huang SM, Mishina YM, Liu S, Cheung A, Stegmeier F, Michaud GA, Charlat O, Wiellette E, Zhang Y, Wiessner S, Hild M, Shi X, Wilson CJ, Mickanin C, Myer V, Fazal A, Tomlinson R, Serluca F, Shao W, Cheng H, Shultz M, Rau C, Schirle M, Schlegl J, Ghidelli S, Fawell S, Lu C, Curtis D, Kirschner MW, Lengauer C, Finan PM, Tallarico JA, Bouwmeester T, Porter JA, Bauer A, Cong F (2009) Tankyrase inhibition stabilizes axin and antagonizes Wnt signalling. Nature 461(7264):614–620

Hurtado de Mendoza T, Balana B, Slesinger PA, Verma IM (2011) Organotypic cerebellar cultures: apoptotic challenges and detection. J Vis Exp (51):e2564 doi:10.3791/2564

Imada S, Murata Y, Kotani T, Hatano M, Sun C, Konno T, Park JH, Kitamura Y, Saito Y, Ohdan H, Matozaki T. 2016. Role of Src family kinases in regulation of intestinal epithelial homeostasis. Mol Cell Biol 36(22):2811–2823

Kerman BE, Kim HJ, Padmanabhan K, Mei A, Georges S, Joens MS, Fitzpatrick JA, Jappelli R, Chandross KJ, August P, Gage FH (2015) In vitro myelin formation using embryonic stem cells. Development 142(12):2213–2225

Lee Y, Morrison BM, Li Y, Lengacher S, Farah MH, Hoffman PN, Liu Y, Tsingalia A, Jin L, Zhang PW, Pellerin L, Magistretti PJ, Rothstein JD (2012) Oligodendroglia metabolically support axons and contribute to neurodegeneration. Nature 487(7408):443–448

Lee HK, Chaboub LS, Zhu W, Zollinger D, Rasband MN, Fancy SP, Deneen B (2015) Daam2-PIP5K is a regulatory pathway for Wnt signaling and therapeutic target for remyelination in the CNS. Neuron 85(6):1227–1243

Maldonado PP, Angulo MC (2015) Multiple modes of communication between neurons and oligodendrocyte precursor cells. Neuroscientist 21(3):266–276

Nave KA (2010) Myelination and support of axonal integrity by glia. Nature 468(7321):244–252

Nave KA, Werner HB (2014) Myelination of the nervous system: mechanisms and functions. Annu Rev Cell Dev Biol 30:503–533

O'Meara RW, Ryan SD, Colognato H, Kothary R (2011) Derivation of enriched oligodendrocyte cultures and oligodendrocyte/neuron myelinating co-cultures from post-natal murine tissues. J Vis Exp (54):e3324. doi:10.3791/3324

Pallen CJ (2003) Protein tyrosine phosphatase alpha (PTPalpha): a Src family kinase activator and mediator of multiple biological effects. Curr Top Med Chem 3(7):821–835

Pedraza CE, Monk R, Lei J, Hao Q, Macklin WB (2008) Production, characterization, and efficient transfection of highly pure oligodendrocyte precursor cultures from mouse embryonic neural progenitors. Glia 56(12):1339–1352

Ponniah S, Wang DZ, Lim KL, Pallen CJ (1999) Targeted disruption of the tyrosine phosphatase PTPalpha leads to constitutive downregulation of the kinases Src and Fyn. Curr Biol 9(10):535–538

Rossol-Allison J, Stemmle LN, Swenson-Fields KI, Kelly P, Fields PE, McCall SJ, Casey PJ, Fields TA (2009) Rho GTPase activity modulates Wnt3a/beta-catenin signaling. Cell Signal 21(11):1559–1568

Sap J, D'Eustachio P, Givol D, Schlessinger J (1990) Cloning and expression of a widely expressed receptor tyrosine phosphatase. Proc Natl Acad Sci U S A 87(16):6112–6116

Sharifi K, Ebrahimi M, Kagawa Y, Islam A, Tuerxun T, Yasumoto Y, Hara T, Yamamoto Y, Miyazaki H, Tokuda N, Yoshikawa T, Owada Y (2013) Differential expression and regulatory roles of FABP5 and FABP7 in oligodendrocyte lineage cells. Cell Tissue Res 354(3): 683–695

Simons M, Trajkovic K (2006) Neuron-glia communication in the control of oligodendrocyte function and myelin biogenesis. J Cell Sci 119(Pt 21):4381–4389

Su J, Muranjan M, Sap J (1999) Receptor protein tyrosine phosphatase alpha activates Src-family kinases and controls integrin-mediated responses in fibroblasts. Curr Biol 9(10):505–511

Tiran Z, Peretz A, Sines T, Shinder V, Sap J, Attali B, Elson A (2006) Tyrosine phosphatases epsilon and alpha perform specific and overlapping functions in regulation of voltage-gated potassium channels in Schwann cells. Mol Biol Cell 17(10):4330–4342

Wang PS, Wang J, Xiao ZC, Pallen CJ (2009) Protein tyrosine phosphatase alpha (PTP{alpha}) acts as an upstream regulator of Fyn signaling to promote oligodendrocyte differentiation and myelination. J Biol Chem 284:33692–33702

Wang PS, Wang J, Zheng Y, Pallen CJ (2012) Loss of protein-tyrosine phosphatase alpha (PTPalpha) increases proliferation and delays maturation of oligodendrocyte progenitor cells. J Biol Chem 287(15):12529–12540

Williams KE, Bundred NJ, Landberg G, Clarke RB, Farnie G (2015) Focal adhesion kinase and Wnt signaling regulate human ductal carcinoma in situ stem cell activity and response to radiotherapy. Stem Cells 33(2):327–341

Xie C, Li Z, Zhang GX, Guan Y (2014) Wnt signaling in remyelination in multiple sclerosis: friend or foe? Mol Neurobiol 49(3):1117–1125

Ye H, Zhao T, Tan YL, Liu J, Pallen CJ, Xiao ZC (2011) Receptor-like protein-tyrosine phosphatase alpha enhances cell surface expression of neural adhesion molecule NB-3. J Biol Chem 286(29):26071–26080

Zeng L, D'Alessandri L, Kalousek MB, Vaughan L, Pallen CJ (1999) Protein tyrosine phosphatase alpha (PTPalpha) and contactin form a novel neuronal receptor complex linked to the intracellular tyrosine kinase fyn. J Cell Biol 147(4):707–714

Zhang H, Jarjour AA, Boyd A, Williams A (2011) Central nervous system remyelination in culture—a tool for multiple sclerosis research. Exp Neurol 230(1):138–148